



**Biobased homopolymers and amphiphilic diblock copolymers containing guaiacyl (G) or hydroxyphenyl (H) lignin derivatives synthesized by RAFT (PISA)**

Journal:	<i>Polymer Chemistry</i>
Manuscript ID	PY-ART-09-2022-001221.R1
Article Type:	Paper
Date Submitted by the Author:	04-Nov-2022
Complete List of Authors:	Balarezo, Mauricio; Sorbonne University Coumes, Fanny; Sorbonne Université, Chemistry Department Stoffelbach, François; Sorbonne University,



Journal Name

ARTICLE

## Biobased homopolymers and amphiphilic diblock copolymers containing guaiacyl (G) or hydroxyphenyl (H) lignin derivatives synthesized by RAFT (PISA)

Received 00th January 20xx,  
Accepted 00th January 20xx

DOI: 10.1039/x0xx00000x

www.rsc.org/

Mauricio Balarezo, Fanny Coumes\* and François Stoffelbach\*

In this work, we exploited guaiacyl (G) and hydroxyphenyl (H) lignin derivatives, namely 4-vinylguaiacol (4-hydroxy-3-methoxystyrene) and *p*-hydroxystyrene, to engineer biobased homopolymers and amphiphilic diblock copolymers. Firstly, after adequate monomers protection, we obtained two homopolymers, poly(acetoxy-protected 4-vinyl guaiacol) (PACVG) and poly(*p*-acetoxy-styrene) (PACST) by reversible addition-fragmentation chain transfer (RAFT) radical polymerization. We characterized their thermal properties and compared them with fossil-fuel-based polystyrene. Then, we used the RAFT-mediated aqueous emulsion polymerization induced self-assembly (PISA) technique to synthesize amphiphilic biobased diblock copolymers from potentially biobased hydrophilic macromolecular chain transfer agents (macroRAFT) based on poly(acrylic acid). We extended the macroRAFTs with each lignin derivative, targeting different degrees of polymerization for the hydrophobic block. The diblock copolymers formation was confirmed by size exclusion chromatography (SEC), while the physico-chemical properties of the *in situ* formed nanoparticles were determined by dynamic light scattering (DLS), (cryogenic) transmission electron microscopy ((cryo-)TEM) and small-angle X-ray scattering spectroscopy (SAXS). Colloidally stable, submicrometric spherical particles composed of the diblock copolymers are formed for all compositions with tuneable diameter. These new biobased latexes, obtained by a RAFT-mediated aqueous emulsion PISA process, pave the way for the formation of a new class of biobased paints, coatings or adhesives.

### Introduction

Over the past decades, the need to develop polymers using a sustainable or eco-friendly approach has increased significantly. One of the strategies employed to produce greener polymers and replace commodity fossil fuel-based polymers is to exploit the available biomass feedstocks. Among these feedstocks, several types of natural polymers such as starch, rubber, (hemi)cellulose and lignin are directly available. The latter, which has been a waste product of the paper industry for a long time, is now in the spotlight and is the subject of much research for its valorization in various industrial applications.<sup>1,2</sup> While extracted lignin can directly be used to generate polymer blends<sup>3</sup> or lignin-based graft copolymers<sup>4</sup>, a lot of research has also been devoted to the depolymerization and recovery of lignin-derived aromatic compounds (LDACs).<sup>5–8</sup> Thus, for more than a decade now, the techniques and synthetic pathways employed to successfully recover these multifunctional LDACs (such as aldehydes, phenols and carboxylic acid precursors) have been developed considerably.<sup>9,10</sup> Many researchers have been interested in their potential to design new biobased polymers. Among aldehydes residues, the most well-known

example is the versatile molecular vanillin platform,<sup>11–14</sup> which allows the formation of biobased polymers and networks through various chemical modifications. Other alternatives derived from cinnamic acid, ferulic acid, sinapic acid and caffeic acid have also been developed, allowing the access to radically polymerizable monomers containing catechyl (C),<sup>15–17</sup> guaiacyl (G),<sup>18–27</sup> syringyl (S)<sup>21,22,28–30</sup> and hydroxyphenyl (H)<sup>21,22,31,32</sup> units and their biobased polymer counterparts.

In order to synthesize well-defined LDACs-biobased homopolymers and block copolymers, we decided herein to use the reversible addition-fragmentation chain transfer (RAFT) radical polymerization technique<sup>33–35</sup> due to its tolerance to a broad range of reaction conditions and monomer families. We then combined it with the polymerization induced self-assembly (PISA) technique to achieve the synthesis of amphiphilic diblock copolymers and the simultaneous formation of self-stabilized nanoparticles (NPs) under green conditions. Combining RAFT-PISA in water with the use of bio-based monomers would allow the preparation of highly concentrated bio-based block copolymer nano-objects. We selected poly(acrylic acid) (PAA) (whose monomer can be easily synthesized from renewable resources<sup>36–39</sup>) as a hydrophilic macromolecular chain transfer agent (macroRAFT) to promote and control the aqueous emulsion polymerization of acetoxy-protected 4-vinylguaiacol and *p*-hydroxystyrene. While the synthesis of LDACs-based polymers by free and controlled radical polymerization in solution<sup>22,23</sup> or emulsion<sup>19</sup> conditions

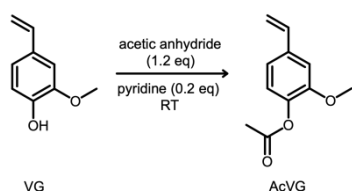
Sorbonne Université, CNRS, UMR 8232, Institut Parisien de Chimie Moléculaire (IPCM), Polymer Chemistry Team, 4 place Jussieu, 75252 Paris Cedex 05, France.  
E-mail: francois.stoffelbach@sorbonne-universite.fr,  
fanny.coumes@sorbonne-universite.fr  
Electronic Supplementary Information (ESI) available. See DOI: 10.1039/x0xx00000x

has already been reported in the literature, to the best of our knowledge, there is no example reporting the synthesis of amphiphilic diblock copolymers using such LDACs in a RAFT-mediated PISA process. Recently, our group reported the first successful synthesis of fully biobased copolymer nanoparticles using PISA process under dispersion conditions in an ecofriendly solvent mixture.<sup>40</sup> Therefore, we describe herein for the first time a RAFT-mediated PISA of LDACs-monomers under aqueous emulsion conditions.

## Results and discussion

### VG protection

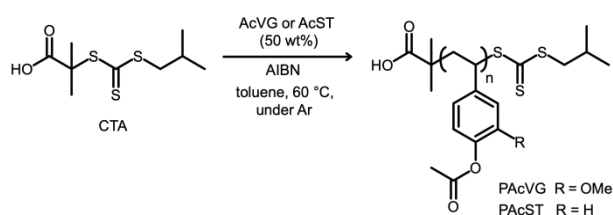
Prior to the radical polymerization, the hydroxyl functionality present in the selected biobased monomers must be protected to avoid unwanted radical quenching during polymerization.<sup>41</sup> While *p*-hydroxystyrene was purchased already protected, acetylation of 4-vinylguaiacol (VG) was performed, according to a modified protocol previously described in the literature<sup>23</sup>, in bulk at room temperature using acetic anhydride in the presence of a catalytic amount of pyridine to yield the desired acetylated 4-vinylguaiacol (AcVG, **Scheme 1**).



**Scheme 1.** Synthesis route of AcVG.

The product was obtained in fairly high yield (>70%) and purity, as evidenced by <sup>1</sup>H NMR. Indeed, the <sup>1</sup>H NMR spectrum of AcVG recorded in CDCl<sub>3</sub> displays the characteristic signals of the vinyl, methoxy and acetoxy groups of the monomer (see **Figure S1**).

### RAFT radical homopolymerization of AcVG and AcST



**Scheme 2.** RAFT radical homopolymerization of AcVG or AcST.

Before using the protected LDACs-monomers in the PISA process proceeding under heterogeneous conditions, we first investigated their ability to be individually radically polymerized in a controlled fashion by RAFT solution polymerization using a trithiocarbonate (TTC) chain transfer agent (CTA) (**Scheme 2**). The polymerizations were performed in toluene at a rather high monomer concentration (50 wt%) in the presence of 4,4'-azobisisobutyronitrile (AIBN) as a radical initiator, keeping the initial CTA/initiator molar ratio constant at 5 and targeting a degree of polymerization (DP) of 60. The two homopolymers were recovered by precipitation and analyzed by <sup>1</sup>H NMR and

size exclusion chromatography (SEC). The results are listed in **Table 1**. A good correlation between the theoretical and experimental molar masses -determined by <sup>1</sup>H NMR- was observed for the two homopolymers. Looking at the SEC chromatograms presented in **Figure S2**, narrow distributions with low dispersities ( $\mathcal{D} < 1.2$ ) were observed despite a slight shoulder towards the higher molar mass side, probably due to bimolecular termination reaction. Thermal analysis by differential scanning calorimetry (DSC) showed that the  $T_g$  of both homopolymers remained in the same temperature range of about 100 °C compared with native polystyrene (PS)<sup>42,43</sup>, which tends to prove that these biobased homopolymers could be used in similar applications (**Figure S3A and Table 1**). In addition, both *samples A1 and A2* displayed similar thermal properties in terms of degradation onset (**Figure S3B**,  $T_{\text{onset}} > 220$  °C) compared to native PS, confirming the interest in using such biobased polymers as an alternative to PS.

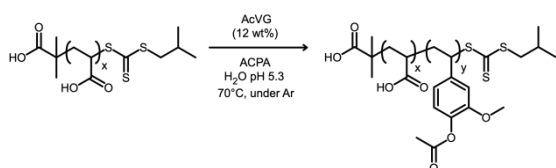
### Synthesis of amphiphilic block copolymers

**Synthesis of macroRAFT PAA-TTC.** To synthesize amphiphilic diblock copolymers through the PISA process in water, we needed a hydrophilic macroRAFT agent. Poly(acrylic acid) (PAA) was selected by targeting two different DP (25 and 50), in order to evaluate the influence of the hydrophilic block length on the polymerization process and the NP's stability. Thus, we first performed solution polymerizations of AA in 1,4-dioxane at 70 °C in presence of the CTA and 4,4'-azobis(4-cyanopentanoic acid) (ACPA) as radical initiator (**Scheme S1**). After 3-4 hours of reaction, the macroRAFT agents were purified by precipitation and lyophilisation and then analyzed by <sup>1</sup>H NMR and SEC (**Table S1**). In both cases, a good correlation between theoretical and experimental molar masses was obtained, as well as monomodal distributions and low dispersities (**Figure S4**).

**Synthesis of PAA-*b*-PacVG: optimization of the emulsion polymerization conditions.** As a first step, we evaluated the possibility of synthesizing amphiphilic diblock copolymers possessing a PAA-based hydrophilic block and a PacVG hydrophobic block using the PISA technique under emulsion polymerization conditions. It has already been shown that the pH of the aqueous medium during emulsion polymerization of hydrophobic monomers using PAA -a pH-sensitive polymer- is of great importance to ensure polymerization control and stabilization of the newly formed NPs in situ.<sup>44</sup> We therefore performed a series of experiments targeting a DP of 50 for PacVG, using the PAA<sub>50</sub>-TTC (M1) macroRAFT agent, where we varied the pH of the reaction medium between 3.0 and 6.3 (below and above the  $pK_a$  5.7 of PAA)<sup>45</sup>. The results are listed in **Table 2**. On the one hand, this series of experiments highlighted that the polymerizations conducted at low pH allowed a better control of the polymerization process, with monomodal distributions and low dispersities ( $\mathcal{D} < 1.2$ ) while being detrimental to the NPs stability since high coagulum content was obtained. On the other hand, a higher pH leads to a better stability of the NPs but a loss of polymerization control occurs. Indeed, at pH 6.3, we observe a bimodal distribution

corresponding to unreacted PAA-TTC, along with uncontrolled polymer chains (**Figure S5**) probably due to the low blocking efficiency at this pH. In order to keep a good polymerization control and NPs stability, we chose to perform the following experiments at pH 5.3.

**PAA-*b*-PacVG through aqueous emulsion PISA: influence of the block's length.** It is now well established that during the PISA process, the morphology of the NPs, mainly spheres, worms/fibers or vesicles, is mainly determined by the block lengths, which affects the packing parameter.<sup>46–48</sup> Thus, we investigated the emulsion polymerization of AcVG from two macroRAFT agents PAA<sub>50</sub>-TTC (M1) and PAA<sub>25</sub>-TTC (M2) respectively, targeting a DP for the hydrophobic block between 50 and 300 (**scheme 3**).



**Scheme 3.** Synthesis route for the preparation of PAA-*b*-PacVG diblock copolymers via RAFT-mediated emulsion PISA in water at pH 5.3 ( $x = 25$  or  $50$  and  $y = 50$  to  $300$ ).

The results are presented in **Table 3**. In general, in all experiments, high monomer conversions ( $\geq 96\%$ ) were reached. SEC chromatograms obtained for the methylated polymers indicate the extension of PAA-TTC to PAA-*b*-PacVG diblock copolymers, as shown in **Figure 1**. Both overlays confirm the synthesis of block copolymers, with the shift of the signals to higher molar masses for each targeted DP. However, we can note the presence of residual macroRAFT in the polymers due to an incomplete extension. Indeed, the blocking efficiency is less than 100% in all cases (see **Table 3**) and decreases as the targeted DP increases for the PAA<sub>25</sub>-TTC macroRAFT, which is not the case with the PAA<sub>50</sub>-TTC macroRAFT. Interestingly, it appears that for the shortest PAA block, dispersities were higher with a slightly more pronounced tailing towards lower molar masses. This could be explained by the length of the macroRAFT which might be too short ( $DP_n = 25$ ) to properly promote and control the polymerization of AcVG under emulsion conditions.

As shown in the photographs (**Figures 1C and 1D**), with increasing DP of the hydrophobic block, the appearance of the solutions changed slightly towards more opaque dispersions, which remained colloidal stable.

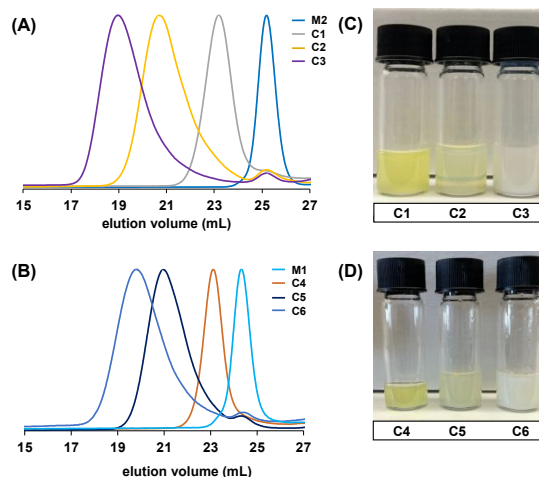


**Figure 1.** Normalized RI SEC chromatograms in THF of methylated macroRAFT agent (PAA<sub>25</sub>-TTC (M2)) and PAA<sub>25</sub>-*b*-PacVG copolymers C1, C2, C3 obtained by PISA at pH = 5.3 (A) and methylated macroRAFT agent (PAA<sub>50</sub>-TTC (M1)) and PAA<sub>50</sub>-*b*-PacVG copolymers C4, C5, C6 obtained by PISA at pH = 5.3 (B). Photographs showing the macroscopic aspect of the final polymerization media (C) and (D).

After removal and quantification of the coagulum (less than 10 wt%), dispersions were diluted at 1 wt% in water and studied by dynamic light scattering (DLS) to determine the particle diameters (**Figure 2A and 2B**). As reported in **Table 3** and shown in **Figure 2C**, by increasing the chain length of the hydrophobic block (DP ranging from 50 to 300), the particle diameter of the final dispersions increased almost linearly from 20 to 60–85 nm.

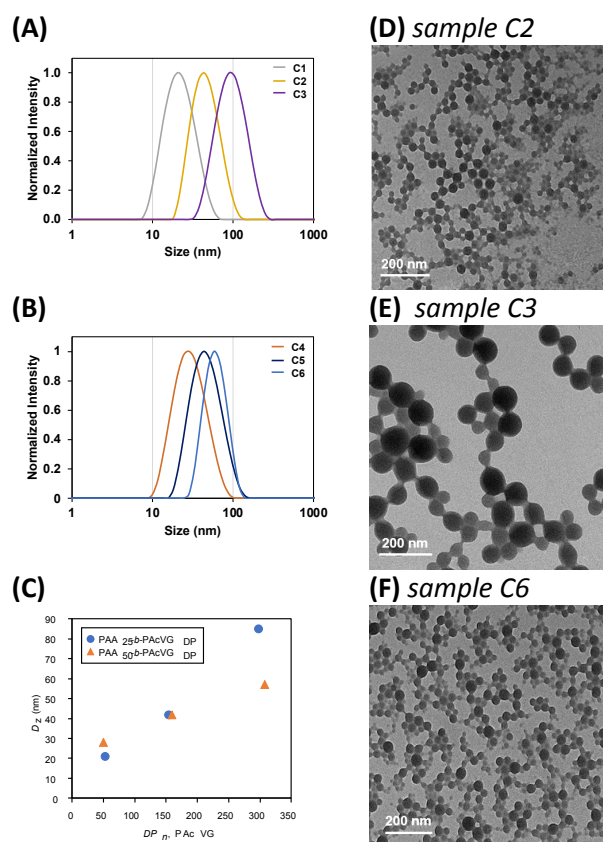
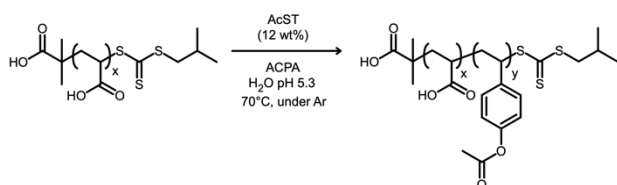


**Figure 2.** Normalized size distributions determined by DLS at 1 wt% in water for dispersions C1 to C3 (A) and C4 to C6 (B). Z-average particle diameter ( $D_z$ ) as a function

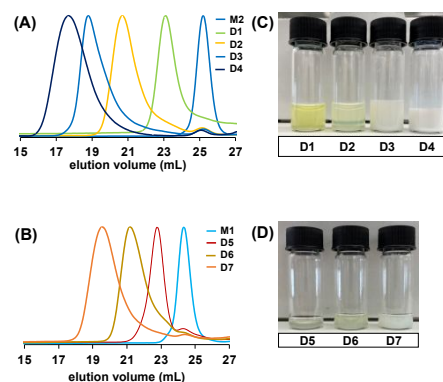
of the hydrophobic block length,  $DP_{n, \text{PACVG}}$  from PAA<sub>25</sub>-TTC (M2) (circle) and PAA<sub>50</sub>-TTC (M1) (triangle) (C). Representative TEM images prepared at room temperature for samples C2 (PAA<sub>25</sub>-*b*-PACVG<sub>151</sub>) (D), C3 (PAA<sub>25</sub>-*b*-PACVG<sub>287</sub>) (E) and C6 (PAA<sub>50</sub>-*b*-PACVG<sub>298</sub>) (F) from latexes diluted at 0.2 wt%.

Surprisingly, for *sample C3* -compared to *sample C6*- a higher  $Z$ -average particle diameter,  $D_z$  was obtained, probably due to coalescence of individual particles due to insufficient stabilization when the hydrophobic block length is too high. TEM experiments of samples C2, C3 and C6 revealed the formation of spherical particles, with diameters smaller than 80 nm (TEM images in **Figure 2**). As previously observed by DLS, an increase in sphere diameter with the hydrophobic block length was observed by TEM measurements. However, no higher order morphology, e.g. worms or vesicles, was observed, as with PAA-*b*-PS diblock copolymers synthesized under comparable conditions.<sup>44,49</sup> Despite this observation, these biobased latexes, which remained stable for more than a year, remain attractive for paints, coatings or adhesives applications.<sup>50,51</sup>

**Synthesis of PAA-*b*-PACST from PAA<sub>25</sub>-TTC or PAA<sub>50</sub>-TTC.** Based on the previous results, we also performed the extension of the both PAA-TTC macroRAFT agents with AcST under emulsion conditions at pH 5.3 (**Scheme 4**). In addition, using the PAA<sub>25</sub>-TTC (M2, Table S1) macroRAFT, we chose to target a higher DP (600) for the AcST block in order to investigate the stability limits of these latexes (**Table 4**). The size exclusion chromatograms in **Figures 3A** and **3B** revealed the formation of a block copolymer, with molar mass dispersities below 1.6 as long as a DP  $\leq 150$  was targeted (**Table 4**). However, significant tailing toward the lower molar mass side was observed. Moreover, dispersity increased as the DP of the hydrophobic block increased, presumably due to side reactions, such as irreversible transfer reactions, which have a greater impact on the  $DP_n$  when high DP values are targeted. For all latexes, a very low amount of coagulum was observed ( $\leq 3$  wt%), indicating a good colloidal stability of the dispersions. As shown in the photographs (**Figures 3C** and **3D**), with increasing DP of the hydrophobic block, the appearance of the solutions changed to milkier dispersions, which remained colloidal stable. As reported in **Table 4** and shown in **Figure S6C**, by increasing the chain length of the hydrophobic block (DP ranging from 50 to 300), the particle diameter of the final dispersions also increased quasi-linearly in the same diameter range compared to the dispersions containing PAA-*b*-PACVG diblock copolymers (for DP ranging from 50 to 300).



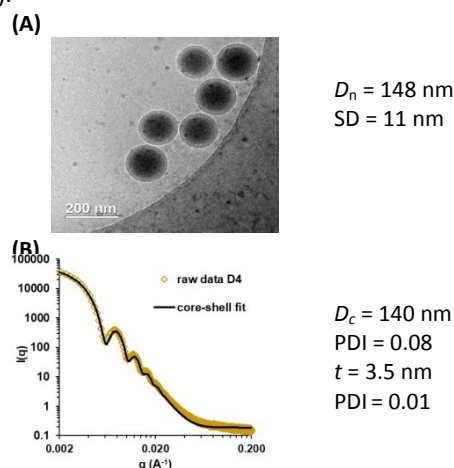
**Scheme 4.** Synthesis route for the preparation of PAA-*b*-PACST diblock copolymers via RAFT-mediated emulsion PISA in water at pH 5.3 ( $x = 25$  or  $50$  and  $y = 50$  to  $540$ ).



**Figure 3.** Normalized size exclusion chromatograms (RI) in THF of methylated macroRAFT agent (PAA<sub>25</sub>-TTC (M2)) and PAA<sub>25</sub>-*b*-PACST copolymers D1 to D4 obtained by PISA at pH = 5.3 (A) and methylated macroRAFT agent (PAA<sub>50</sub>-TTC (M1)) and PAA<sub>50</sub>-*b*-PACST copolymers D5 to D7 obtained by PISA at pH = 5.3 (B). Photographs showing the macroscopic aspect of the final polymerization media (C) and (D).

The dispersions were diluted at 0.2 wt% in water and studied by TEM to determine the particles morphology. Only spheres were again observed with an increase of the sphere diameter with the hydrophobic block length (**Figure S7**).

Interestingly, when the *sample D4* was analysed by cryo-TEM (**Figure 4A**), the core-shell structure of the NPs could be observed, which was not the case by TEM (**Figure S7C**) probably due to the dehydration of the shell. This core-shell feature was confirmed by small-angle X-ray scattering (SAXS) spectroscopy experiments. Indeed, from the scattering profile, displayed in **Figure 4B**, a core-shell spherical model of NPs was fitted with diameter dimensions close to those obtained by cryo-TEM and DLS. Furthermore, this scattering profile, with multiple oscillations confirms the presence of core-shell NPs with a low dispersity in diameters, as visually observed by cryo-TEM on **Figure 4A**. A similar core-shell feature was also observed for *sample D3* by cryo-TEM (**Figure S8A**) and was confirmed by SAXS (**Figure S8B**), but with higher dispersity (no oscillations observed).



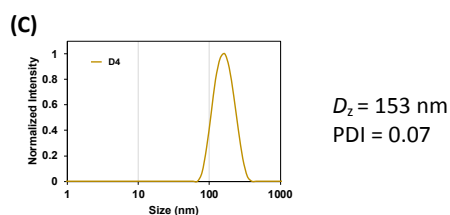


**Figure 4.** (A) Representative cryo-TEM image of *sample D4* (diluted at 1 wt%) with  $D_n$ , the number-average diameter determined on 20 representative nano-objects and  $SD$ , the standard deviation. (B) SAXS profiles of *sample D4* (diluted 1 wt%) with  $D_c$ , the core diameter and  $t$ , the shell thickness using a sphere core-shell model and a lognormal distribution. (C) Normalized size distribution determined by DLS at 1 wt% in water for dispersion D4 with  $D_z$ , the Z-average particle diameter. PDI = polydispersity index.

## Conclusion

In this work, we were able to exploit guaiacyl (G) and hydroxyphenyl (H) lignin derivatives to engineer biobased homopolymers and amphiphilic diblock copolymers. Indeed, homopolymers of acetoxy-protected 4-vinylguaiacol (AcVG) and *p*-hydroxystyrene (AcST) were prepared with good control by the RAFT technique using a trithiocarbonate RAFT agent. The homopolymers showed similar properties to polystyrene in terms of  $T_g$  and thermal stability, confirming the interest in using such biobased polymers as alternatives for PS polymers. Then, two series of PAA-*b*-PACVG and PAA-*b*-PACST biobased amphiphilic diblock copolymers with different degrees of polymerization for both blocks were prepared by RAFT-mediated emulsion PISA in water. In order to keep good polymerization control and colloidal stability of the dispersion, we demonstrated that the polymerization should be performed at pH 5.3. We also demonstrated that no influence of the hydrophobic block length (DP between 50 to 300) on the morphology of the self-assemblies was observed by TEM, only spherical nanoparticles were formed whose diameter increased from 20 to 150 nm with the increase of the DP of PACVG or PACST. These new biobased latexes, obtained by a RAFT-mediated aqueous emulsion PISA process, pave the way for the formation of a new class of biobased paints, coatings or adhesives. In addition, deprotection of acetoxy groups<sup>17</sup> can lead to phenolic functions in polymers, which may be interesting for future applications.

## Experimental

### Materials and methods

All the reagents were purchased from Sigma-Aldrich and used without further purification unless otherwise noted. The RAFT agent (CTA) was synthesized according to a protocol previously described in the literature.<sup>52</sup> Acrylic acid (AA, Aldrich, 99%), was distilled under vacuum prior to polymerization. All aqueous solutions were prepared with deionized water. All syntheses and polymerizations were conducted under argon atmosphere. **Nuclear Magnetic Resonance (NMR).**  $^1\text{H}$  NMR spectra were recorded in DMSO- $d_6$ , THF- $d_8$  or  $\text{CDCl}_3$  at 300 K on a Bruker 300 MHz spectrometer in 5 mm diameter tubes.

**Size exclusion chromatography (SEC).** SEC measurements were carried out to determine the number-average molar mass ( $M_n$ ), the weight-average molar mass ( $M_w$ ), and the dispersity ( $D = M_w/M_n$ ) on three PL Gel Mixte C 5  $\mu\text{m}$  columns ( $7.5 \times 300$  mm; separation limits: 0.2 to 2000  $\text{kg}\cdot\text{mol}^{-1}$ ) maintained at 40 °C coupled with a solvent and sample delivery module Viscotek GPCmax and a differential refractive index (RI) detector Viscotek 3580 calibrated with polystyrene standards (PS, from Polymer Standards Services). THF was used as the mobile phase at a flow rate of 1  $\text{mL}\cdot\text{min}^{-1}$  and toluene was used as a flow rate marker. All polymers were injected (100  $\mu\text{L}$ ) at a concentration of 5  $\text{mg}\cdot\text{mL}^{-1}$  after filtration through a 0.45  $\mu\text{m}$  pore-size membrane. The OmniSEC 5.12 software was used for data acquisition and data analysis. Polymers containing AA units have been modified by methylation of the carboxylic acid groups using trimethylsilyldiazomethane before SEC analysis.<sup>53</sup>

**Dynamic Light Scattering (DLS)** measurements were carried out on a Zetasizer Nano S90 from Malvern (90° angle, 5 mW He-Ne laser at 633 nm) to determine the Z-average particle diameter ( $D_z$ ) of diluted dispersions in water at 1 wt% concentration (unless stated differently).

**pH measurements.** The pH value of the aqueous dispersions was probed by a pH-meter (Mettler Toledo DL50 Graphix) using a micro-pH electrode (Mettler Toledo DGi101-SC).

**Differential scanning calorimetry (DSC)** measurements were performed on a TA instruments Q2000 device. Heating-cooling cycles were successively performed between 0 and 150 °C at a rate of 20 °C $\cdot\text{min}^{-1}$  under  $\text{N}_2$ .

**Thermogravimetry analysis (TGA)** measurements were performed using a TA instruments Q50 to assess the resistance towards degradation of homopolymers (PACVG and PACST).

**Transmission Electron Microscopy (TEM)** images were obtained by diluting the sample in ultra-pure water at 0.2 wt%. A volume of 3  $\mu\text{L}$  was deposited on the grid and left to dry at ambient temperature. Images of particles were observed by a JEOL JEM 2011 microscope operating at 200 kV. The images were taken on a Gatan Orius CCD Camera.

**Cryogenic Transmission Electron Microscopy (cryo-TEM)** analyses: polymer solution was prepared at 1 wt% in ultra-pure water (unless otherwise stated). 3  $\mu\text{L}$  of the solution was then deposited on a quantifoil grid. After removing the excess of solution with a Whatman paper, the grid was immediately frozen in liquid ethane. The observations were carried out at -180 °C by a JEOL JEM-2100 LaB<sub>6</sub> microscope operating at 200 kV. The images were taken on a Gatan US 1000, 2k by 2k CCD Camera.

**Small-angle X-ray scattering (SAXS).** Selected samples (D3 and D4) were analyzed by SAXS measurements on the SWING beamline of the SOLEIL Synchrotron (Saint Aubin, France). The measurements were performed at an energy of 12 keV ( $\lambda = 1.03$  Å), with an exposure time of 1000 ms and a gap time of 500 ms and measured by a two-dimensional CCD detector localized at a distance of 3500 mm from the sample to achieve a low  $q$ -range detection. Standard correction procedures were applied for X-ray beam transmission, signal subtraction of the 1.5 mm capillary filled with the solvent and detector efficiency.

The software *Foxtrot*<sup>®</sup> and *SasView*<sup>®</sup> were used to achieve such data reduction. **Fit of the SAXS data.** The data was fitted with the *SasView* software (<http://www.sasview.org/>). According to the observed morphologies using cryo-TEM, the data were fitted with the form factor of a lognormal distribution of spheres.

### Synthetic procedures

**Synthesis of AcVG.** VG (6.0 g, 40.0 mmol) was introduced in a round bottom flask under argon and cooled down in an ice bath. Acetic anhydride (4.4 mL, 46.7 mmol) and pyridine (0.8 mL, 9.9 mmol) were progressively added while stirring. The reaction proceeded for 2h at RT. Diethyl ether (100 mL) was added to the mixture and the solution was washed twice with HCl (100 mL, 10<sup>-4</sup> M) and once with distilled water (100 mL). The organic phase was dried over MgSO<sub>4</sub> and the solvent was evaporated under vacuum, giving a colourless viscous oil (5.51 g, 72%).

<sup>1</sup>H NMR CDCl<sub>3</sub> (300 MHz, δ): 6.99 (m, 2H), 6.68 (dd, 1H), 5.70 (d, 1H), 5.24 (d, 1H), 3.86 (s, 3H), 2.31 (s, 3H).

**General procedure for the RAFT homopolymerization of AcVG and AcST.** In a typical experiment (Table 1, entry A2), AcST (1.88 mL, 12.3 mmol, 60 eq.), CTA (52 mg, 0.21 mmol, 1eq.), AIBN (6.7 mg, 0.04 mmol, 0.2 eq.) and toluene (2.24 mL) were placed in a 5 mL round-bottom flask equipped with a magnetic stirrer. The solution was purged with argon for 10 min in an ice bath. The flask was then placed in a thermostated oil bath at 60 °C. After 31.5h, the polymerization was quenched by exposing to air and immersing in an ice bath. The polymer was precipitated twice in diethyl ether. The recovered yellow powder was dried overnight under vacuum at 40 °C.

**General procedure for the synthesis of macroRAFT PAA-TTC.** The preparation of macroRAFT PAA-TTC was adapted from the literature.<sup>53</sup> In a typical experiment (Table S1, entry M1), in a 50 mL ice-cooled round bottom-flask equipped with a magnetic stirrer containing degassed solution of ACPA (26.8 mg, 96 μmol, 0.1 eq.), CTA (0.24 g, 0.97 mmol, 1 eq.) and trioxane (added as an internal reference for the determination of the monomer consumption by <sup>1</sup>H NMR) in 1,4-dioxane (26 mL), acrylic acid (3.8 mL, 55.6 mmol, 57 eq.) was introduced. The mixture was degassed 5 min prior to immersion of the flask in a thermostated oil bath at 70 °C. Aliquots were taken from the reaction media and analyzed by <sup>1</sup>H NMR to determine the monomer conversion. Polymerization was quenched upon reaching conversion of 85%. The polymer was recovered as a yellow powder after purification by precipitation in cold diethyl ether. It was then dried under reduced pressure and finally lyophilised.

**General procedure for the synthesis of PAA-*b*-PACVG or PAA-*b*-PACST diblock copolymers by RAFT-mediated emulsion PISA in water.** In a typical experiment (Table 4, entry D5), 0.86 mL of an aqueous solution of ACPA (2.6 mg, 9.3 μmol, 0.3 eq., neutralised by 2 eq. of NaHCO<sub>3</sub>) and 0.86 mL of an aqueous solution of PAA-TTC (Table S1, entry M1, 0.12 g, 0.03 mmol, 1 eq.) were placed in a 2 mL round-bottom flask. The pH was adjusted to 5.3 using

NaHCO<sub>3</sub>. AcST (0.24 mL, 1.57 mmol, 51 eq.) was added into the reaction mixture. The emulsion was purged with argon for 10 min in an ice bath before being immersed in thermostated oil bath at 70 °C. Aliquots were periodically withdrawn to follow the conversion by <sup>1</sup>H NMR. Polymerization was quenched after reaching conversion higher than 95%. Coagulum was separated from the latex by centrifugation (3 times 5 min at 3200 rpm). It was then washed and dried 2h in the oven at 60 °C to determine the weight percentage with respect to the copolymer.

### Author Contributions

Project administration: F.S.; Conceptualization / Supervision / validation / Writing review & editing: F.S. and F.C.; Investigation Data curation: M.B.; Writing- original draft: M.B and F.C.

### Conflicts of interest

There are no conflicts to declare.

### Acknowledgements

We thank SOLEIL for the provision of synchrotron radiation facilities. We are grateful to Dr. Thomas Bizien for assistance in using the “swing” beamline (proposal number 20220204) and to the SOLEIL staff for smoothly running the facility. This work benefited from the use of the *SasView* application, originally developed under NSF award DMR-0520547. *SasView* contains code developed with funding from the European Union’s Horizon 2020 research and innovation program under the SINE2020 project, grant agreement No 654000. We also thank Clément Debrie for data SAXS treatments and Jean-Michel Guigner for the cryo-TEM analyses.

### Notes and references

- V. Yadav, A. Kumar, M. Bilal, T. A. Nguyen and H. M. N. Iqbal, in *Nanotechnology in Paper and Wood Engineering*, eds. R. Bhat, A. Kumar, T. A. Nguyen and S. Sharma, Elsevier, 2022, pp. 265–283.
- I. Haq, P. Mazumder and A. S. Kalamdhad, *Bioresour. Technol.*, 2020, **312**, 123636.
- E. Lizundia, M. H. Sipponen, L. G. Greca, M. Balakshin, B. L. Tardy, O. J. Rojas and D. Puglia, *Green Chem.*, 2021, **23**, 6698–6760.
- H. Liu, L. Mulderrig, D. Hallinan and H. Chung, *Macromol. Rapid Commun.*, 2021, **42**, 2000428.
- G. F. Bass and T. H. Epps, *Polym. Chem.*, 2021, **12**, 4130–4158.
- R. C. Rajak, P. Saha, M. Singhvi, D. Kwak, D. Kim, H. Lee, A. R. Deshmukh, Y. Bu and B. S. Kim, *Green Chem.*, 2021, **23**, 5584–5599.
- R. Behling, S. Valange and G. Chatel, *Green Chem.*, 2016, **18**, 1839–1854.
- J. Karthäuser, V. Biziks, C. Mai and H. Miltz, *Molecules*, 2021, **26**, 2533.
- S. Fadlallah, P. Sinha Roy, G. Garnier, K. Saito and F. Allais, *Green Chem.*, 2021, **23**, 1495–1535.
- Q. Mei, X. Shen, H. Liu and B. Han, *Chin. Chem. Lett.*, 2019, **30**, 15–24.

- 11 M. Fache, B. Boutevin and S. Caillol, *Eur. Pol. J.*, 2015, **68**, 488–502.
- 12 M. Fache, E. Darroman, V. Besse, R. Auvergne, S. Caillol and B. Boutevin, *Green Chem.*, 2014, **16**, 1987–1998.
- 13 A.-S. Mora, R. Tayouo, B. Boutevin, G. David and S. Caillol, *Green Chem.*, 2018, **20**, 4075–4084.
- 14 Q. Yu, X. Peng, Y. Wang, H. Geng, A. Xu, X. Zhang, W. Xu and D. Ye, *Eur. Pol. J.*, 2019, **117**, 55–63.
- 15 T. Hirai, J. Kawada, M. Narita, T. Ikawa, H. Takeshima, K. Satoh and M. Kamigaito, *Polymer*, 2019, **181**, 121667.
- 16 H. Takeshima, K. Satoh and M. Kamigaito, *ACS Sustainable Chem. Eng.*, 2018, **6**, 13681–13686.
- 17 S. Tanizaki, T. Kubo and K. Satoh, *Macro Chemistry & Physics*, 2022, **223**, 2100378.
- 18 H. Takeshima, K. Satoh and M. Kamigaito, *Polymers*, 2018, **10**, 1404.
- 19 W. S. J. Li, V. Ladmiral, H. Takeshima, K. Satoh, M. Kamigaito, M. Semsarilar, C. Negrell, P. Lacroix-Desmazes and S. Caillol, *Polym. Chem.*, 2019, **10**, 3116–3126.
- 20 T. M. McGuire, M. Miyajima, M. Uchiyama, A. Buchard and M. Kamigaito, *Polym. Chem.*, 2020, **11**, 5844–5850.
- 21 H. Takeshima, K. Satoh and M. Kamigaito, *J. Polym. Sci.*, 2020, **58**, 91–100.
- 22 J. van Schijndel, D. Molendijk, K. van Beurden, L. A. Canalle, T. Noël and J. Meuldijk, *Eur. Polym. J.*, 2020, **125**, 109534.
- 23 H. Takeshima, K. Satoh and M. Kamigaito, *Macromolecules*, 2017, **50**, 4206–4216.
- 24 S. Molina-Gutiérrez, V. Ladmiral, R. Bongiovanni, S. Caillol and P. Lacroix-Desmazes, *Ind. Eng. Chem. Res.*, 2019, **58**, 21155–21164.
- 25 S. Molina-Gutiérrez, A. Manseri, V. Ladmiral, R. Bongiovanni, S. Caillol and P. Lacroix-Desmazes, *Macromol. Chem. Phys.*, 2019, **220**, 1900179.
- 26 S. Molina-Gutiérrez, W. S. J. Li, R. Perrin, V. Ladmiral, R. Bongiovanni, S. Caillol and P. Lacroix-Desmazes, *Biomacromolecules*, 2020, **21**, 4514–4521.
- 27 A.-B. Al-Odayni, W. S. Saeed, A. Y. B. H. Ahmed, A. Alrahlah, A. Al-Kahtani and T. Aouak, *Polymers*, 2020, **12**, 160.
- 28 A. Galano, M. Francisco-Márquez and J. R. Alvarez-Idaboy, *J. Phys. Chem. B*, 2011, **115**, 8590–8596.
- 29 K. L. Morley, S. Grosse, H. Leisch and P. C. K. Lau, *Green Chem.*, 2013, **15**, 3312.
- 30 A. L. Holmberg, K. H. Reno, N. A. Nguyen, R. P. Wool and T. H. Epps, *ACS Macro Lett.*, 2016, **5**, 574–578.
- 31 R. Fernandez-Alvarez, E. Hlavatovičová, K. Rodzeń, A. Strachota, S. Kereiche, P. Matějček, J. Cabrera-González, R. Núñez and M. Uchman, *Polym. Chem.*, 2019, **10**, 2774–2780.
- 32 B. Gao, X. Chen, B. Iván, J. Kops and W. Batsberg, *Macromol. Rapid Commun.*, 1997, **18**, 1095–1100.
- 33 J. Chiefari, Y. K. (Bill) Chong, F. Ercole, J. Krstina, J. Jeffery, T. P. T. Le, R. T. A. Mayadunne, G. F. Meijs, C. L. Moad, G. Moad, E. Rizzardo and S. H. Thang, *Macromolecules*, 1998, **31**, 5559–5562.
- 34 C. Barner-Kowollik and S. Perrier, *J. Polym. Sci. A Polym. Chem.*, 2008, **46**, 5715–5723.
- 35 C. Barner-Kowollik, in *Handbook of RAFT Polymerization*, John Wiley & Sons, Ltd, 2008, pp. 1–4.
- 36 P. Boontawan, S. Kanchanathawee and A. Boontawan, *Biochem. Eng. J.*, 2011, **54**, 192–199.
- 37 X. Zhang, L. Lin, T. Zhang, H. Liu and X. Zhang, *Chem. Eng. J.*, 2016, **284**, 934–941.
- 38 T. Pirman, M. Ocepek and B. Likozar, *Ind. Eng. Chem. Res.*, 2021, **60**, 9347–9367.
- 39 J. G. H. Hermens, A. Jensma and B. L. Feringa, *Angew. Chem. Int. Ed.*, 2022, **61**, e202112618.
- 40 F. Coumes, M. Balarezo, J. Rieger and F. Stoffelbach, *Macromol. Rapid Commun.*, 2020, **41**, 2000002.
- 41 F. Lartigue-Peyrou, in *Industrial Chemistry Library*, Elsevier, 1996, vol. 8, pp. 489–505.
- 42 J. Rieger, *J. Therm. Anal.*, 1996, **46**, 965–972.
- 43 G. Reiter, M. Sferrazza and P. Damman, *Eur. Phys. J. E*, 2003, **12**, 133–138.
- 44 I. Chaduc, A. Crepet, O. Boyron, B. Charleux, F. D’Agosto and M. Lansalot, *Macromolecules*, 2013, **46**, 6013–6023.
- 45 E. Velasquez, J. Rieger, F. Stoffelbach, F. D’Agosto, M. Lansalot, P.-E. Dufils and J. Vinas, *Polymer*, 2016, **106**, 275–284.
- 46 J. N. Israelachvili, D. J. Mitchell and B. W. Ninham, *J. Chem. Soc., Faraday Trans. 2*, 1976, **72**, 1525.
- 47 A. Blanazs, S. P. Armes and A. J. Ryan, *Macromol. Rapid Commun.*, 2009, **30**, 267–277.
- 48 J. Rieger, *Macromol. Rapid Commun.*, 2015, **36**, 1458–1471.
- 49 F. Coumes, F. Stoffelbach and J. Rieger, in *Macromolecular Engineering*, John Wiley & Sons, Ltd, 2022, pp. 1–84.
- 50 W. Liu, S. Zhang, Q. Li, X. Li and H. Wang, *J Appl Polym Sci*, 2019, **136**, 47463.
- 51 A. Badía, A. Agirre, M. J. Barandiaran and J. R. Leiza, *Biomacromolecules*, 2020, **21**, 4522–4531.
- 52 X.-P. Qiu, F. Tanaka and F. M. Winnik, *Macromolecules*, 2007, **40**, 7069–7071.
- 53 E. Velasquez, G. Pembouong, J. Rieger, F. Stoffelbach, O. Boyron, B. Charleux, F. D’Agosto, M. Lansalot, P.-E. Dufils and J. Vinas, *Macromolecules*, 2013, **46**, 664–673.

**Table 1. Experimental conditions and results for the RAFT-mediated homopolymerizations of AcVG and AcST performed in toluene**

Sample	M	[M] <sub>0</sub> (M)	Time (h)	Conv. <sup>a</sup> (%)	$M_{n,th}^b$ (kg·mol <sup>-1</sup> )	$DP_{n,NMR}^c$	$M_{n,NMR}^c$ (kg·mol <sup>-1</sup> )	$M_{n,SEC}^d$ (kg·mol <sup>-1</sup> )	$\mathcal{D}^d$	$T_g^e$ (°C)	$T_{deg}^f$ (°C)
A1	AcVG	4.6	23	80	9.3	44	8.7	6.4	1.14	104	220
A2	AcST	5.5	32	64	6.4	40	6.7	6.0	1.08	105	220

All polymerizations were carried out at 60 °C, at an initial monomer concentration of 50 wt% using AIBN as a radical initiator with an initial molar ratio,  $n_{monomer,0} / n_{AIBN,0} / n_{CTA,0} = 60/0.2/1$ . <sup>a</sup> Determined by <sup>1</sup>H NMR in CDCl<sub>3</sub>. <sup>b</sup> Theoretical number-average molar mass,  $M_{n,th}$ , determined *via* the monomer conversion. <sup>c</sup> Number-average degree of polymerization,  $DP_{n,NMR}$ , and number-average molar mass,  $M_{n,NMR}$ , determined by <sup>1</sup>H NMR from chain-end. <sup>d</sup> Number-average molar mass and dispersity,  $\mathcal{D}$ , determined by SEC in THF with a PS calibration. <sup>e</sup> Determined using DSC measurements, 2<sup>nd</sup> heating. <sup>f</sup> Determined using TGA measurements, onset of significant degradation.

**Table 2. Experimental conditions and results for the RAFT-mediated emulsion PISA of AcVG in water at different pH in the presence of PAA<sub>50</sub>-TTC as a macromolecular RAFT agent**

Sample	pH	Time (h)	Conv. <sup>a</sup> (%)	$DP_{n,th}^b$	$M_{n,th}^b$ (kg·mol <sup>-1</sup> )	$M_{n,SEC}^c$ (kg·mol <sup>-1</sup> )	$\mathcal{D}^c$	Coag. <sup>d</sup> (wt%)	$D_z^e$ (nm) (PDI)
B1	3.0	2	97	49	13.2	10.1	1.13	15	-
B2	4.4	5	99	50	13.4	11.6	1.27	6	34 (0.30)
B3	5.3	7	100	50	13.5	10.7	1.17	2	28 (0.25)
B4	6.3	4	100	50	13.3	70.9	1.65	5	87 (0.05)

All polymerizations were carried out at 70 °C, at an initial monomer concentration of 12 wt% using ACPA as a radical initiator with an initial molar ratio,  $n_{monomer,0} / n_{ACPA,0} / n_{macroRAFT,0} = 50/0.3/1$ . <sup>a</sup> Determined by <sup>1</sup>H NMR in DMSO-d<sub>6</sub>. <sup>b</sup> Theoretical number-average degree of polymerization,  $DP_{n,th}$  (PACVG), and number-average molar mass,  $M_{n,th}$ , calculated using the experimental conversion. <sup>c</sup> Number-average molar mass ( $M_n$ ) and dispersity ( $\mathcal{D}$ ) determined by SEC in THF for the methylated copolymers using a polystyrene calibration and recalculated for the nonmethylated ones. <sup>d</sup> Weight percentage of coagulum with respect to copolymer. <sup>e</sup>  $D_z$  is the Z-average particle diameter and PDI the polydispersity index derived from dynamic light scattering determined at 1 wt% in water.

**Table 3. Experimental conditions and results for the RAFT-mediated emulsion PISA of AcVG in water at pH 5.3 in the presence of PAA<sub>25</sub> or <sub>50</sub>-TTC as a macromolecular RAFT agent**

Sample	[M] <sub>0</sub> /[ACPA] <sub>0</sub> / [PAA-TTC] <sub>0</sub>	Time (h)	Conv. <sup>a</sup> (%)	$DP_{n,th}^b$	$M_{n,th}^b$ (kg·mol <sup>-1</sup> )	$M_{n,SEC}^c$ (kg·mol <sup>-1</sup> )	$\mathcal{D}^c$	Blocking efficiency <sup>d</sup> (%)	Coag. <sup>e</sup> (wt%)	$D_z^f$ (nm) (PDI)	$D_n^g$ (nm)
<b>MacroRAFT PAA<sub>25</sub>-TTC (M2)</b>											
C1	53/0.3/1	6	97	51	11.9	7.5	1.50	85	7	21 (0.24)	-
C2	154/0.3/1	4	98	151	31.1	34.7	1.67	43	9	42 (0.10)	39
C3	298/0.3/1	3	96	287	57.3	102.4	1.88	32	3	85 (0.17)	75
<b>MacroRAFT PAA<sub>50</sub>-TTC (M1)</b>											
C4 (B3 in Tab. 2)	50/0.3/1	7	100	50	13.5	10.7	1.17	81	2	28 (0.25)	-
C5	160/0.3/1	6	99	159	34.2	32.7	1.46	74	6	42 (0.13)	-
C6	307/0.3/1	4	97	298	61.0	66.0	1.78	77	6	57 (0.09)	44

All polymerizations were carried out at 70 °C and at an initial monomer concentration of 12 wt% using ACPA as a radical initiator. <sup>a</sup> Determined by <sup>1</sup>H NMR in THF-d<sub>8</sub>. <sup>b</sup> Theoretical number-average degree of polymerization,  $DP_{n,th}$  (PACVG), and number-average molar mass,  $M_{n,th}$ , calculated using the experimental conversion. <sup>c</sup> Number-average molar mass ( $M_n$ ) and dispersity ( $\mathcal{D}$ ) determined by SEC in THF for the methylated copolymers using a polystyrene calibration and recalculated for the nonmethylated ones. <sup>d</sup> Blocking efficiency determined according to the method described in the SI. <sup>e</sup> Weight percentage of coagulum with respect to copolymer. <sup>f</sup>  $D_z$  is the Z-average particle diameter and PDI the polydispersity index derived from dynamic light scattering determined at 1 wt% in water (The respective correlograms are shown in Figure S10). <sup>g</sup>  $D_n$  = number-average diameter determined on 35 representative nano-objects by TEM at 0.2 wt% in water.

**Table 4.** Experimental conditions and results for the RAFT-mediated emulsion PISA of AcST in water at pH 5.3 in the presence of PAA<sub>25</sub> or PAA<sub>50</sub>-TTC as a macromolecular RAFT agent

Sample	[AcST] <sub>0</sub> /[ACPA] <sub>0</sub> / [PAA-TTC] <sub>0</sub>	Time (h)	Conv. <sup>a</sup> (%)	DP <sub>n,th</sub> <sup>b</sup>	M <sub>n,th</sub> <sup>b</sup> (kg·mol <sup>-1</sup> )	M <sub>n,SEC</sub> <sup>c</sup> (kg·mol <sup>-1</sup> )	Đ <sup>c</sup>	Blocking efficiency <sup>d</sup> (%)	Coag. <sup>e</sup> (wt%)	D <sub>z</sub> <sup>f</sup> (nm) (PDI)	D <sub>n</sub> <sup>g</sup> (nm)
<b>MacroRAFT PAA<sub>25</sub>-TTC (M2)</b>											
D1	50/0.3/1	7	100	50	10.4	9.1	1.23	79	2	20 (0.23)	-
D2	152/0.3/1	6	96	146	25.8	34.8	1.52	47	1	35 (0.08)	29
D3	301/0.3/1	6	97	292	49.5	97.3	1.92	24	1	80 (0.09)	75
D4	597/0.3/1	7	90	537	89.0	254.7	1.96	10	1	153 (0.07)	152
<b>MacroRAFT PAA<sub>50</sub>-TTC (M1)</b>											
D5	51/0.3/1	7	100	51	12.1	12.5	1.21	74	2	29 (0.17)	-
D6	153/0.3/1	7	98	150	28.0	28.2	1.39	74	2	35 (0.16)	25
D7	305/0.3/1	6	97	296	51.8	71.0	1.74	77	3	57 (0.08)	38

All polymerizations were carried out at 70 °C and at an initial monomer concentration of 12 wt% using ACPA as a radical initiator. <sup>a</sup> Determined by <sup>1</sup>H NMR in THF-d<sub>8</sub>. <sup>b</sup> Theoretical number-average degree of polymerization, DP<sub>n,th</sub> (PACST), and number-average molar mass, M<sub>n,th</sub>, calculated using the experimental conversion. <sup>c</sup> Number-average molar mass (M<sub>n</sub>) and dispersity (Đ) determined by SEC in THF for the methylated copolymers using a polystyrene calibration and recalculated for the nonmethylated ones. <sup>d</sup> Blocking efficiency determined according to the method described in the SI. <sup>e</sup> Weight percentage of coagulum with respect to copolymer. <sup>f</sup> D<sub>z</sub> is the Z-average particle diameter and PDI the polydispersity index derived from dynamic light scattering determined at 1 wt% in water (The respective correlograms are shown in Figure S11). <sup>g</sup> D<sub>n</sub> = number-average diameter determined on 35 representative nano-objects by TEM at 0.2 wt% in water.